Proc. of the 32nd International Symposium on Shock Waves (ISSW32)
doi:10.3850/978-981-11-2730-4_0501-cd

Shock Wave Moderation by Characterized Disturbances

A. Sasoh and A. Iwakawa
Department of Aerospace Engineering, Nagoya University, Furo-cho, Chikusa-ku, Nagoya 464-8603, Japan

Akihiro Sasoh: akihiro.sasoh@mae.nagoya-u.ac.jp

Abstract Shock waves behave their interesting characteristic when interacting with various fluctuations. In this paper, shock wave behaviors influenced by controlled disturbances, thermal bubble, turbulence and boundary layer are discussed based on experimental results. Also, their applications to aerospace engineering will be suggested.

1 Introduction

Many of compressible fluid dynamics problems are solved based on the so-called Riemann problem, in which two uniform regions sharing an interface evolve according to one-dimensional mass, momentum and energy conservation relations. If a region the condition of which is controlled by external momentum and/or energy input interacts with a shock wave, the solution of the Riemann problem can evolve in various ways. In this paper, we present some examples of shock wave moderation owing to such interactions.

2 One-Dimensional Riemann Problem

Figure 1 shows the x(space)-t(time) diagram of a Riemann problem. Initially, two uniform regions, the left (L) and right (R) regions contacts each other by a contact surface. After the interaction starts, either a shock wave or an expansion fan propagates in the respective regions so that new states L* and R*, that are separated by the contact surface are formed. Across the contact surface, the pressure and flow velocity do not vary, yet the temperatures and densities on the respective sides do not necessarily equal to each other. If we wisely utilize the characteristics of a solution of Riemann problem, we will obtain important and useful applications.

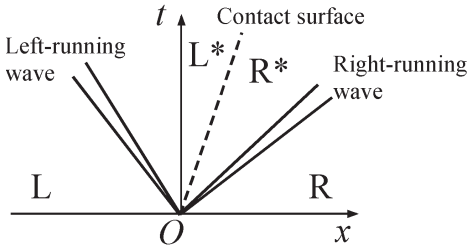

Fig. 1 Wave diagram of the Riemann problem in general form

3 Shock-Thermal Bubble Interaction

When a shock wave interacts with a low density/high temperature region, the acoustic impedance is lower than that of the intact state, the shock is weakened due to generation of an expansion fan. Moreover, counter flow against the shock propagation direction is generated,

decreasing the wave drag[1-15]. A laser pulse is irradiated on to a small spot so that optical breakdown and following electron avalanche follow. The emitted free electrons absorb the proceeding laser power. As is observed in many applications, this process is almost isochoric. Because the pressure in this laser heated region becomes much higher than that of the surroundings. The media expands to equilibrate the pressure imbalance. After the expansion, a laser-heated, thermal bubble which has a lower density and a higher temperature than those in the surroundings is formed.

Figure 2 shows shadowgraph images of thermal bubble formation in the quiescent, atmospheric air. The pulsed energy was supplied by the Nd:YAG Laser (Nano-T 250, Litron Laser Ltd., pulse energy: 250 mJ maximum, pulse duration: 7 – 10 ns). Through the experiments, the pulse energy was set to 200 mJ. The laser beam was focused by LightPath® Gradium® lens with a focal length of 40 mm, and was introduced in a chamber through the BK7 window. The breakdown was induced in the chamber and was visualized by using z-shaped shadowgraphy. The visualization system was constructed by a pulsed diode laser light source (Cavitar Ltd., CAVILUX Smart, wavelength: 640 nm, pulse duration: 10 ns minimum), a high-speed camera (Ultra8, framing rate: 100 Mfps, image size: 682 × 682 pixels, 12-bit monochrome color, nac Image Technology Inc.), and a pair of concave mirrors. Prior to the experiment, the delay time of the laser irradiation to induced breakdown was measured and the repeatability of the phenomena of the laser-induced breakdown was confirmed. The images from 50 ns before breakdown to 4,000 ns after breakdown were obtained per 10 ns through the series of the experiments. The origin of the time, t, is set to the moment when the image of the laser-heated bubble is first captured. **Error! Reference source not found.** shows the initial state of the laser-induced breakdown. The resolution of the image was 0.08 mm/pixel, hence the diameter of the initial bubble was $d_0 = 2.8$ mm. This bubble gradually expanded and the bubble size became as twice the initial size after 3,950 ns from the laser irradiation, see Fig. 2(b). The bright ring is the blast wave induced by the laser breakdown. The terminal size of the bubble is 70 pixels, which equals $d_1 = 5.6$ mm. Assuming isentropic expansion, the energy absorption efficiency is evaluated to be 0.25.

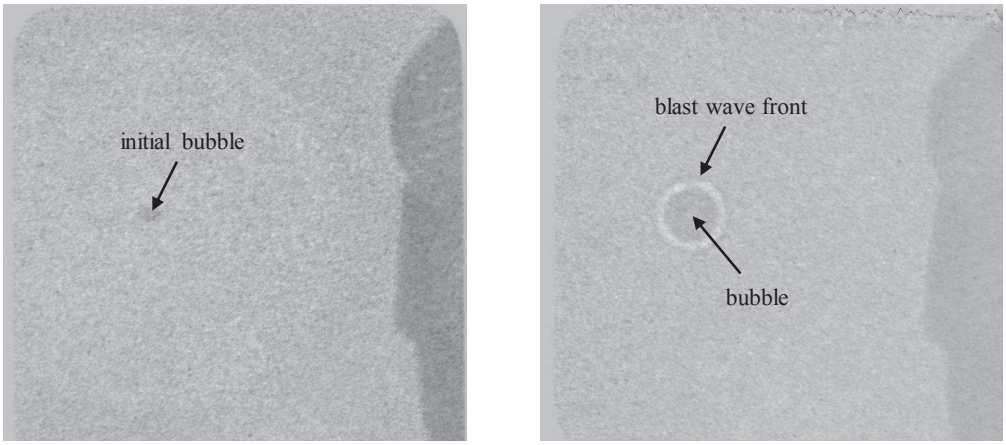

(a) $t = 0$ ns (b) $t = 3950$ ns

Fig. 2 Visualization of thermal bubble formation in quiescent, atmospheric air

Figure 3 schematically illustrates the interaction between the thermal bubble and a shock wave formed ahead of a blunt body. By Galilean transformation from the laboratory coordinate to the coordinate on the shock wave, this interaction is reduced to a Riemann problem, in which the shock transmits in the bubble and expansion fan propagates in the post-shock region.

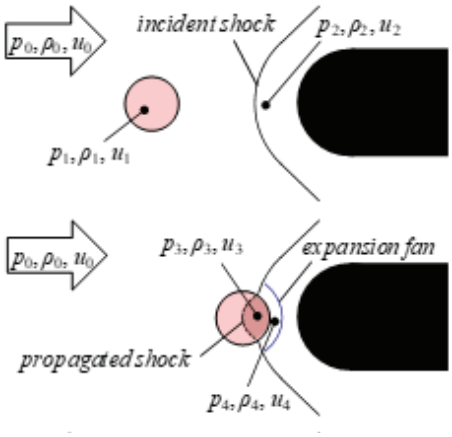

Fig. 3 Schematic illustration of shock wave and thermal bubble interaction

In the experiment shown in Fig. 4, the thermal bubble diameter before the interaction with the shock wave is $d_1 = 3.8$ mm. **Error! Reference source not found.**5 compares the experimentally-measured shock wave motion with that obtained by numerical simulation.

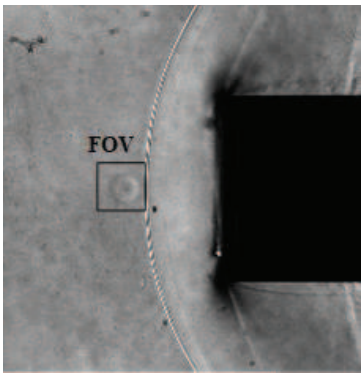

Fig.4 Schlieren snapshot before shock-bubble interaction in Mach-1.92 wind tunnel.

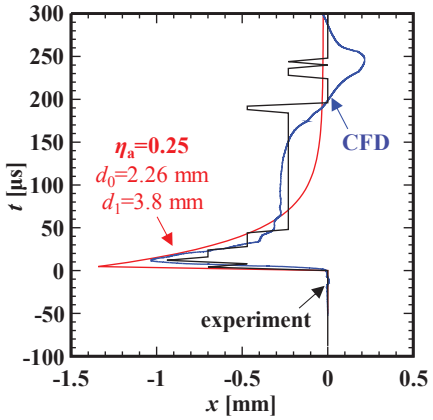

Fig. 5 Shock wave motion after single pulse energy deposition in the experiment shown in Fig. 4.

The impacts of the interaction with the thermal-bubble on the wave drag reduction was documented in Refs. 2-15.

4 Shock-Turbulence Interaction

Interaction between a shock wave and turbulence is an important and fundamental problem, and involves in many applications including sonic boom modulation by atmospheric turbulence [16-18]. In spite of intensive efforts of numerical investigations [19-26], experimental data are necessary. Past experimental works used various configurations of a shock wave and turbulence [27-36]. The most fundamental configuration is the interaction between a plane shock wave and canonical turbulence. However, this configuration is difficult to be implemented experimentally. In order to realize this configuration, experimental investigations using a shock tube were done [37-42]. In those experiments, the shock Mach number and the turbulent Mach number were not controlled in an independent manner. In order to conduct systematic experiment on shock wave-turbulence interaction, we have developed a small, counter-driver shock tube (CD-ST)[43]. Currently, we have developed a 14-m-long CD-ST with a 120 mm × 120 mm square cross-section.

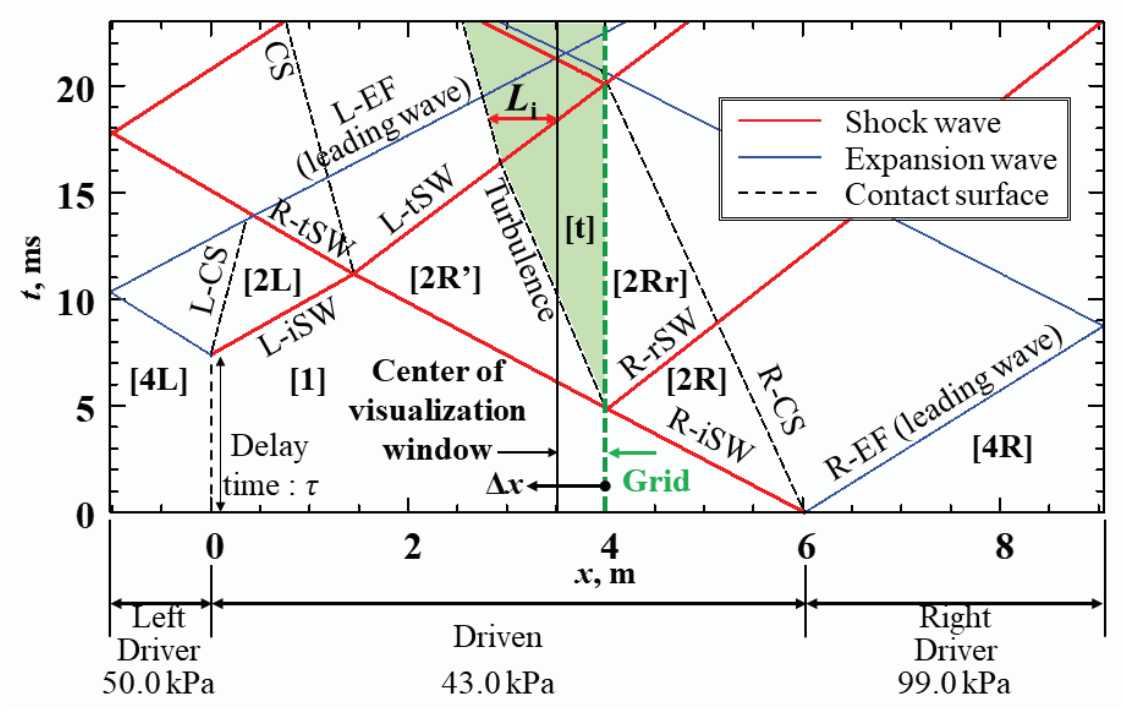

Fig. 6 Example of wave diagram of shock-grid turbulence interaction in a counter-driver shock tube, shock Mach number of L-tSW, 1.04; turbulent Mach number at Δx = 0.45 m, 0.011; L_i, 0.81 m.

Figure 6 shows an example of the CD-ST operation. In this example, the total length of the CD-ST was 10 m. First, the diaphragm at the right driver was ruptured using a needle attached to an electrically-controlled pneumatic cylinder. The incident shock wave, R-iSW, propagates to the left, transmits past the grid at $x = 4.0$ m, behind the shock wave grid turbulence, the green region in Fig. 6, is generated. After a delay time, $\tau = 7.4$ ms, the diaphragm at the left driver was ruptured by using another rupture device of the same type, thereby another incident shock wave, L-iSW, propagates to the right. R-iSW and L-iSW collide against each other, then forming transmitting shock waves, R-tSW and L-tSW, and a contact surface, CS. Then, L-tSW interacts with the grid turbulence in the green region. The interaction length, L_i, is defined as the distance from the shock wave at the center of the visualization window and the leading head of the grid turbulence.

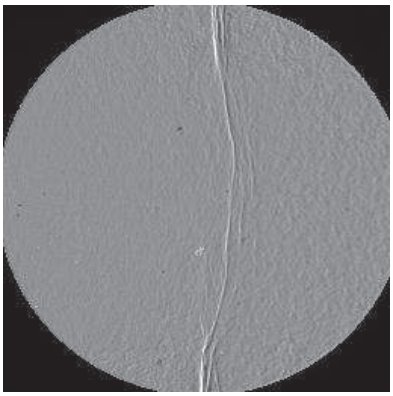

Fig. 7 Shadowgraph images of a shock wave interacting with turbulence, shock Mach number of L-tSW, 1.04; turbulent Mach number at $\Delta x = 0.45$ m, 0.024; $L_i = 781$ mm.

5 Shock-Boundary Layer Interaction

Shock wave-boundary layer interaction is another important, fundamental problem in compressible fluid dynamics [44,45]. If a boundary layer exists on a body in supersonic flows, the inverse pressure gradient propagates back toward the upstream, inducing flow separation and a separation bubble. In front of the bubble, the flow is directed off the wall, accompanied by a separation shock. Behind the bubble, the flow re-attaches with the accompanying compression waves. If the compression waves coalesce, an oblique shock wave appears. In the boundary layer, the flow Mach number varies from 0 (on the wall) to a supersonic value. Under the sonic line, the flow is subsonic, and the shock wave smears out. If such a shock wave-boundary layer interaction is significant in the real flow, the effective streamline changes, possibly degrading the performance of aerodynamic devices.

Experimental and numerical studies have been done on the moderation of shock wave-boundary layer interaction by using energy deposition [46-48]. Figure 8 shows the schlieren images which is colored as post-processing of a Mach-19.2 flow over a hemisphere-cylinder-flare body. Without laser-pulse energy deposition, the flow separates near the cylinder-flare corner, accompanying a separation shock wave appearing even near the hemisphere-cylinder connection. On the other hand, with energy deposition, the flow separation region becomes much smaller, and the separation shock wave becomes much weaker. In this flow, the thermal

bubbles generated by the laser pulse energy depositions decreases the inverse pressure gradient through similar processes as to the shock-bubble interaction. The stronger the separation shock wave, the larger the effect of the energy deposition becomes. However, once the separated flow becomes modified by the energy deposition, its effect becomes weak. This trade-off leads to an optimum power that should be deposited to the flow. Application of the energy deposition to improve supersonic diffuser performance was done in Ref. 49.

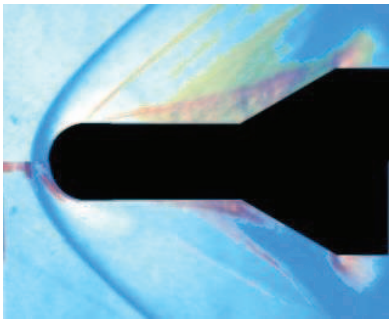

Fig. 8 Colored Schlieren image of shock-boundary layer interaction over a hemisphere-cylinder-flare model, upper, without energy deposition; lower with energy deposition 5.5 mJ/pulse; laser pulse repetition frequency, 60 kHz.

6 Summary and Prospects

Shock wave has fascinating, dynamic, nonlinear nature that it is moderated by even weak disturbances. The stronger a shock wave, the more effective the impact becomes. This nature can be applied to various applications including the improvement of re-visiting, supersonic transportation technology.

References

[1] D. M. Bushnell, *Shock Wave Drag Reduction*, Annual Review of Fluid Mechanics. **3** , 81 (2004)
[2] Knight, D. D., *Survey of Aerodynamic Drag Reduction at High Speed by Energy Deposition*, Journal of Propulsion and Power. **24**, 1153 (2008)
[3] Riggins, D., Nelson, H. F., and Johnson, E., *Blunt-Body Wave Drag Reduction using Focused Energy Deposition*, AIAA Journal. **37**, 460 (1999)
[4] Riggins, D. W., and Nelson, H. F., *Hypersonic Flow Control using Upstream Focused Energy Deposition*, AIAA Journal. **38**, 4 (2000)
[5] Kremeyer, K., Ebastian, K., and Shu, C.-W., *Computational Study of Shock Mitigation and Drag Reduction by Pulsed Energy Lines*, AIAA Journal. **44**, 1720 (2006)
[6] Kandala, R., and Candler, G. V., *Numerical Studies of Laser-Induced Energy Deposition for Supersonic Flow Control*, AIAA Journal. **42**, 2266 (2004)
[7] Kim, J.-H., Matsuda, A., Sakai, T., and Sasoh, A., *Wave Drag Reduction Performance with Acting Spike Induced by Laser-Pulse Energy Depositions*, AIAA Journal. **49**, 2076 (2011)
[8] Tret'yakov, P., Garanin, A., Kraynev, V., Tupikin, A., and Yakovlev, V., *Investigation of local laser energy release influence on supersonic flow by methods of aerophysical experiments*, International Conference on Methods of Geophysical Research 1, (1996)

[9] Adelgren, R. G., Yan, H., Elliott, G. S., Knight, D. D., Beutner, T. J., and Zheltovodov, A. A., *Control of Edney IV Interaction by Pulsed Laser Energy Deposition*, AIAA Journal. **43**, 256 (2005)
[10] Georgievskii, P. Y., and Levin, V. A., *Control of the Flow Past Bodies Using Localized Energy Addition to the Supersonic Oncoming Flow*, Fluid Dynamics. **38**, 794 (2003)
[11] Iwakawa, A., Sakai, T., and Sasoh, A., *Repetition Frequency Dependence of Wave Drag Reduction Induced by Laser-Pulse-Energy Depositions*, Transactions of the Japan Society for Aeronautical and Space Sciences, Aerospace Technology Japan, **11**, 53 (2013)
[12] Markhotok, A., *A mechanism of wave drag reduction in the thermal energy deposition experiments*, Physics of Plasmas. **22**, 063512 (2015)
[13] Azarova, O., "*Supersonic Flow Control Using Combined Energy Deposition*," Aerospace. **2**, 118 (2015)
[14] Rezaei Sangtabi, A., Ramiar, A., Ranjbar, A. A., Abdollahzadeh, M., and Kianifar, A., *Influence of repetitive laser pulse energy depositions on supersonic flow over a sphere, cone and oblate spheroid*, Aerospace Science and Technology. **76**, 72 (2018)
[15] Iwakawa, A., Shoda, T., Majima, R., Pham, S. H. S. H., and Sasoh, A., *Mach Number Effect on Supersonic Drag Reduction using Repetitive Laser Energy Depositions over a Blunt Body*, Transactions of the Japan Society for Aeronautical and Space Sciences. **60**, 303 (2017)
[16] S. K. Lele, *Shock-jump relations in a turbulent flow*, Phys. Fluids 4, 2900 (1992)
[17] H. H. Hubbard, D. J. Maglieri, V. Huckel, and D. A. Hilton, *Ground Measurements of Sonic-Boom Pressures for the Altitude Range of 10,000 to 75,000 feet*, NASA TR R-198 (1964)
[18] E. J. Kane, *Some Effects of the Atmosphere on Sonic Boom*, NASA SP-147, 49 (1967)
[19] S. Lee, S. K. Lele, and P. Moin, *Direct numerical simulation of isotropic turbulence interacting with a weak shock wave*, J. Fluid Mech. **251**, 533 (1993)
[20] J. Larsson and S. K. Lele, *Direct numerical simulation of canonical shock/turbulence interaction*, Phys. Fluids. **21**, 126101 (2009)
[21] D. A. Donzis, *Amplification factors in shock-turbulence interactions: Effect of shock thickness*, Phys. Fluids. **24**, 011705 (2012)
[22] D. A. Donzis, *Shock structure in shock-turbulence interactions*, Phys. Fluids. **24**, 126101 (2012)
[23] Y. Tian, F. A. Jaberi, Z. Li, and D. Livescu, *Numerical study of variable density turbulence interaction with a normal shock wave*, J. Fluid Mech. **829**, 551 (2017)
[24] L. Ryu and D. Livescu, *Turbulence structure behind the shock in canonical shock–vortical turbulence interaction*, J. Fluid Mech. **756**, R1 (2014)
[25] D. Livescu and L. Ryu, *Vorticity dynamics after the shock–turbulence interaction*, Shock Waves. **26**, 241 (2016)
[26] J. Larsson, I. Bermejo-Moreno, and S. K. Lele, *Reynolds- and Mach-number effects in canonical shock-turbulence interaction*, J. Fluid Mech. **717**, 293 (2013)
[27] H. S. Ribner, P. J. Morris, and W. H. Chu, *Laboratory simulation of development of superbooms by atmospheric turbulence*, J. Acoust. Soc. Am. **53**, 3 (1973)
[28] P. E. Roach, *The generation of nearly isotropic turbulence by means of grids*, Int. J. Heat Fluid FL. **8**, 82 (1987)
[29] T. Kitamura, K. Nagata, Y. Sakai, A. Sasoh, O. Terashima, H. Saito, and T. Harasaki, *On invariants in grid turbulence at moderate Reynolds numbers*, J. Fluid Mech. **738**, 378 (2014)
[30] B. Lipkens and D. T. Blackstock, *Model experiment to study sonic boom propagation through turbulence*, J. Acoust. Soc. Am. **103**, 148 (1998)
[31] J.-H. Kim, A. Sasoh, and A. Matsuda, *Modulations of a weak shock wave through a turbulent slit jet*, Shock Waves. **20**, 339 (2010)

[32] T. Tamba, D. Furukawa, Y. Aoki, M. Kayumi, A. Iwakawa, A. Sasoh, T. Matsunaga, M. Izumo, Y. Sugiyama, T. Matsumura, and Y. Nakayama, *Field experiment of blast wave pressure modulation past a turbulent flow*, Sci. Tech. Energetic Mat. **77**, 91 (2016)
[33] A. Sasoh, T. Harasaki, T. Kitamura, D. Takagi, S. Ito, A. Matsuda, K. Nagata, and Y. Sakai, *Statistical behavior of post-shock overpressure past grid turbulence*, Shock Waves. **24**, 489 (2014)
[34] T. Kitamura, K. Nagata, Y. Sakai, A. Sasoh, and Y. Ito, *Changes in divergence-free grid turbulence interacting with a weak spherical shock wave*, Physics of Fluids. **29**, 065114 (2017)
[35] K. Inokuma, T. Watanabe, K. Nagata, A. Sasoh, and Y. Sakai, *Finite response time of shock wave modulation by turbulence*, Phys. Fluids. **29**, 051701 (2017)
[36] S. Barre, D. Alem, and J. P. Bonnet, *Experimental Study of a Normal Shock/Homogeneous Turbulence Interaction*, AIAA J. **34**, 5 (1996)
[37] D. S. Dosanjh, I*nteraction of grids with traveling shock waves*, NACA TN-3680 (1956)
[38] G. Briassulis, J. H. Agui, and Y. Andreopoulos, *The structure of weakly compressible grid-turbulence*, J. Fluid Mech. **432**, 219 (2001)
[39] A. Honkan and J. Andreopoulos, *Rapid compression of grid-generated turbulence by a moving shock wave*, Phys. Fluids A: Fluid Dynamics. **4**, 11 (1992)
[40] A. Honkan, C. B. Watkins, and J. Andreopoulos, *Experimental Study of Interactions of Shock Wave With Free-Stream Turbulence*, J. Fluid Eng. **116**, 4 (1994)
[41] S. Xanthos, G. Briassulis, and Y. Andreopoulos, *Interaction of Decaying Freestream Turbulence with a Moving Shock Wave: Pressure Field*, J. Propul. Power. **18**, 6 (2002)
[42] J. H. Agui, G. Briassulis, and Y. Andreopoulos, *Studies of interactions of a propagating shock wave with a decaying grid turbulence: velocity and vorticity fields*, J. Fluid Mech. **524**, 143 (2005)
[43] T. Tamba, T. M. Nguyen, K. Takeya, T. Harasaki, A. Iwakawa, A. Sasoh, *Counter-driver shock tube*, Shock Waves. **25**, 667 (2015)
[44] Babinsky, H. and Harvey, K. J., *Shock Wave-Boundary-Layer Interactions*, Cambridge Aerospace Series, Cambridge University Press. (2011)
[45] Dolling, S. D., *Fifty Years of Shock-Wave/Boundary-Layer Interaction Research: What Next?*, AIAA Journal. **39**, 1517 (2001)
[46] Osuka, T., Erdem, E., Hasegawa, N., Majima, R., Tamba, T., Yokota, S., Sasoh, A., and Kontis, K., *Laser Energy Deposition Effectiveness on Shock-Wave Boundary-Layer Interactions over Cylinder-Flare Combinations*, Physics of Fluids. **26**, 096103 (2014)
[47] Tamba, T., Pham, H. S., Shoda, T., Iwakawa, A., and Sasoh, A., *Frequency modulation in shock wave-boundary layer interaction by repetitive-pulse laser energy deposition*, Physics of Fluids. **27**, 091704 (2015)
[48] Pham, H., S., Shoda, T., Tamba, T., Iwakawa, A., and Sasoh, A., *Impacts of laser energy deposition on flow instability over double-cone model*, AIAA Journal. **55**, 2992 (2017)
[49] Pham, H., M., Myokan, T., Tamba, T., Iwakawa, A., and Sasoh, A., *Effects of Repetitive Laser Energy Deposition on Supersonic Duct Flows*, AIAA Journal. **56**, 542 (2018)